Inorganic Chemistry

Article

pubs.acs.org/IC

Synthesis, Structure, and Magnetic Studies of Manganese–Oxygen Clusters of Reduced Coordination Number, Featuring an Unchelated, 5-Coordinate Octanuclear Manganese Cluster with Water-Derived Oxo Ligands

Sandeep K. Kondaveeti,[†] Shivaiah Vaddypally,[†] Carol Lam,[†] Daigorou Hirai,[‡] Ni Ni,[‡] Robert J. Cava,*[,‡] and Michael J. Zdilla*[,†]

[†]Department of Chemistry, Temple University, 1901 N. 13th Street, Philadelphia, Pennsylvania 19122, United States

[‡]Department of Chemistry, Princeton University, Princeton, New Jersey 08544, United States

Supporting Information

ABSTRACT: The synthesis of reduced coordination (less than 6), unchelated manganese oxygen cluster systems is described. Addition of phenols to $Mn(NR_2)_2$ (R = $SiMe_3$) results in protolytic amide ligand replacement, and represents the primary entry into the described chemistry. Addition of PhOH to $Mn(NR_2)_2$ results in the formation of the heteroleptic dimer $Mn_2(\mu\text{-}OPh)_2(NR_2)_2(THF)_2$ (**1**). Usage of the sterically larger 2,6-diphenylphenol ($Ph_2C_6H_3OH$) as the ligand source results in the formation of a 3-coordinate heteroleptic dimer without THF coordination, $Mn_2(\mu\text{-}OC_6H_3Ph_2)_2(NR_2)_2$ (**2**). Attempts to generate **2** in the presence of THF or Et_2O resulted in isolation of monomeric $Mn(OC_6H_3Ph_2)_2L_2$ (**3**, L = THF, Et_2O). Use of the sterically intermediate 2,4,6-trimethylphenol (MesOH) resulted in formation of the linear trinuclear cluster $Mn_3(\mu\text{-}OMes)_4(NR_2)_2(THF)_2$ (**4**). Reaction of $Mn(NR_2)_2$ with PhOH in the presence of water, or reaction of **1** with water, results in the formation of a 5-coordinate, unchelated Mn–O cluster, $Mn_8(\mu_5\text{-}O)_2(\mu\text{-}OPh)_{12}(THF)_6$ (**5**). Preparation, structures, steric properties, and magnetic properties are presented. Notably, complex **5** exhibits a temperature-dependent phase transition between a 4-spin paramagnetic system at low temperature, and an 8-spin paramagnetic system at room temperature.

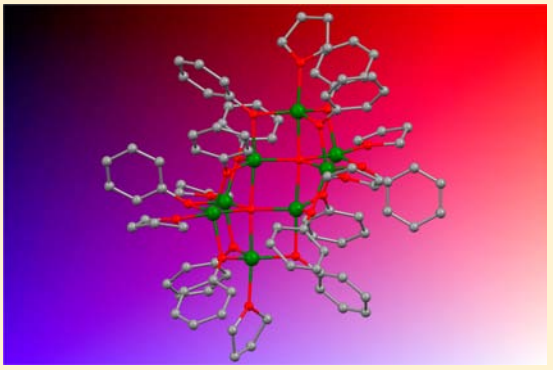

INTRODUCTION

Water oxidation is a grand challenge in the pursuit of renewable solar hydrogen. In nature, water oxidation is achieved by the oxygen evolving complex (OEC) of photosystem II,[1] a Mn_4CaO_5 cluster. The crystal structure of the resting state of this catalyst has recently been determined to 1.9 Å,[2] and is shown in Figure 1. Even before the obtainment of this newest picture of the OEC, elucidation of the nature of the catalyst by biophysical[3] and earlier X-ray crystallographic[4] studies inspired the exploration of synthetic manganese–oxo clusters as biomimetic compounds. The breadth of work on this synthetic chemistry is extensive, and has been reviewed.[5]

A number of reports on manganese–oxo systems are especially worthy of note. Brudvig has reported dimeric and tetrameric manganese–oxo complexes which evolve oxygen.[6] The group of Dismukes has reported an oxygen evolving Mn–O cluster, which has been shown to mediate photocatalytic water splitting when infused into a Nafion membrane, demonstrated through a collaboration with the Spiccia group.[7] This latter cluster is relevant not only for its catalytic activity, but also for its biologically relevant cubane structure.

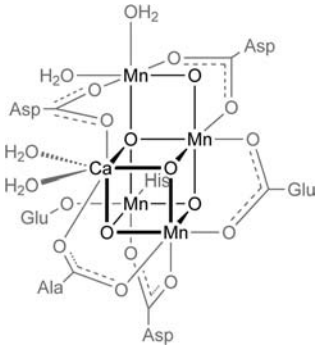

Figure 1. Crystallographic model of the oxygen evolving center (OEC) of photosystem II.[2]

Other cubane motifs have been reported by Christou[8] and by Li[9] which incorporate Ca and Na, respectively, into the cubane motif. Most recently, reports from the laboratories of

Received: November 14, 2011
Published: September 4, 2012

Scheme 1. Preparation of Low-Coordiante, Unchelated Mn−O Clusters

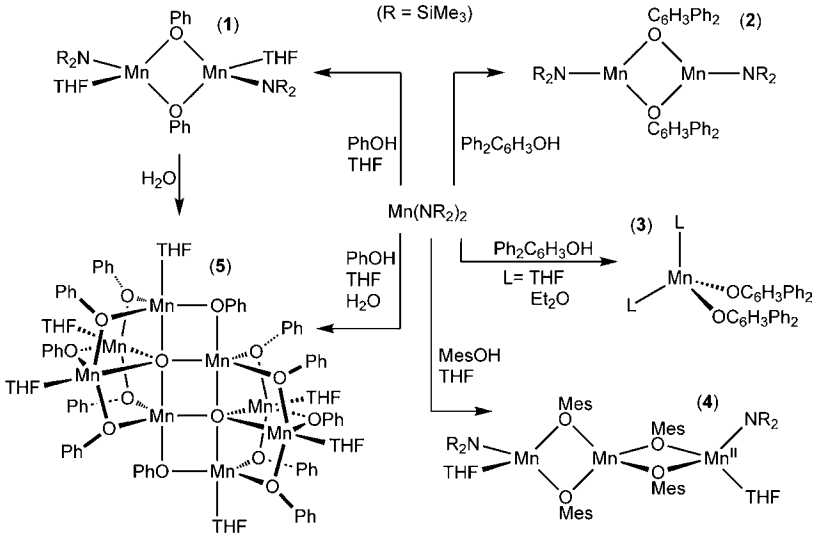

Christou[8c] and Agapie[10] describe the preparation of the most structurally accurate Mn−Ca−O cubanes to date. A Mn−O−Ca complex has also been reported recently by Borovik.[11] Also worthy of note are the Co and Ni systems of Nocera,[12] which represent some of the most promising synthetic water oxidation catalysts so far, and have been proposed to be constructed of metal−oxo cubane motifs.[13]

While there are a few examples of Mn−O systems that exhibit interesting biomimetic reaction chemistry, including some of those above, the vast majority of Mn−O systems are kinetically and thermodynamically inert. This lack of reactivity stems from the stabilization of the complexes by multidentate, octahedral ligation. In the 1.9 Å crystallographic model, the OEC contains a mixture of mono- and bidentate ligands,[2] and undergoes oxidation state-dependent rearrangements according to biophysical studies.[1,3] As in most metalloenzyme systems, significant protein motion can facilitate required active site rearrangement and stabilize transition states and intermediates during enzyme turnover. In contrast, synthetic systems which model the protein environment using multidentate ligation tend to be inert due to the chelate effect. A notable exception is seen in the work of Armstrong, who has reported on a manganese cluster which undergoes a reversible redox-dependent structural change, and which has EPR signatures remarkably similar to the biological system.[14]

Synthetic manganese−oxo cluster systems almost exclusively contain metal sites that are octahedral, which stabilizes the high (active) oxidation states, and precludes water binding. The recent structure at 1.9 Å resolution clearly shows that the "dangler" manganese atom contains but two protein based ligands, and has two bound waters. Synthetic manganese oxo clusters with bound water molecules are rare, and primarily from the Brudvig group.[15] Additionally, recent biophysical EPR studies have concluded that the S_2 state of photosystem II most likely possesses manganese centers with lower-than-six coordination.[16] The control of transition metal coordination number, especially using bulky substituted aromatics, has been pioneered by Phillip Power.[17] Other particularly noteworthy molecular activation by has been seen at iron complexes of reduced coordination number by Holland,[18] at early transition metals by Mindiola,[19] at nickel by Hillhouse,[20] and at Mo and Nb by Cummins.[21] Of particular relevance to the approach presented in this report is the extensive work on metal phenolate chemistry in the literature, with noteworthy contributions from a number of groups.[17,22] With regard to biomimetic chemistry of the OEC, there is impetus for the exploration of reactive manganese−oxo clusters of decreased coordination number.[23]

There are a number of examples of 5-coordinate manganese−oxo dinuclear and trinuclear complexes,[24,25] and numerous examples of clusters with a mixture of 5- and 6-coordination are known,[26] but high-nuclearity Mn−O clusters with exclusive metal coordination number of less than 6 are rare, limited to just a few reports.[27] Of these, tetranuclear Mn clusters with a single central oxide are the most common, with 4 examples.[27a−d] Most noteworthy are a Mn_4O_2 cluster with "butterfly" geometry,[27e] and a Mn_8O_2 cluster containing 4- and 5-coordinate Mn from the group of Wright.[27f] Examples of clusters without multidentate ligands are even more rare, with the only example, to our knowledge, being a Mn_4I_6O cluster.[27d] We report here a number of Mn−OAr based complexes and clusters with 3-, 4-, and 5-coordination formed in the absence of chelating ligands using steric control. Featured is a novel octanuclear Mn−O cluster with exclusively 5-coordinate metals, no chelation, and water-derived bridging oxo ligands.

RESULTS AND DISCUSSION

General. The general strategy of cluster synthesis is protolytic ligand replacement by acidic ligand sources. Addition of an acidic ligand source (e.g., phenol) to a metal precursor containing Brønsted basic ligands with gentle or no heating allows for mild ligand replacement reactions, and circumvents redox side reactions frequently encountered in self-assembled cluster synthesis by ion metathesis.[5,28] For all complexes, bis[bis(trimethylsilyl)amido]manganese(II) ($Mn(NR_2)_2$, R = $SiMe_3$)[29] was used as the manganese source. The protolytically labile NR_2^- ligand is easily replaced by acidic donors. The mild protolytic ligand replacement reaction allows the maintainance of the Mn(II) oxidation state throughout. Thus, the major driving force for the formation of the reported systems is the protonation of the NR_2^- ligand, which results in its dissociation. The open coordination sites are filled by the resulting oxygen-based anionic ligands, and the clusters self-

dx.doi.org/10.1021/ic202448c | Inorg. Chem. 2012, 51, 10095−10104

assemble into the lowest-energy geometry. Results of formation of manganese aryloxide complexes are shown in Scheme 1.

Addition of parent and modified phenols to colorless $Mn(NR_2)_2$ proceeds with a slight darkening of color as the reaction proceeds, though all final products are colorless. Typically, some turbidity is observed, which disappears upon stirring for several minutes. Clear colorless crystals of all such complexes are obtained by vapor diffusion of pentane or hexamethyldisiloxane with a solution of the cluster, or chilling of the concentrated reaction mixture. All complexes were identified and characterized by single-crystal X-ray diffraction and CHN elemental analysis. ^{1}H NMR spectra have been obtained, but exhibit paramagnetically shifted and very broad spectra consistent with high-spin Mn^{II} complexes.

Preparation of Mono-, Di-, and Trinuclear Mn−OAr Complexes and Steric Effects. The addition of 1 equiv of anhydrous phenol to $Mn(NR)_2$ results in protolysis of one amide ligand to extrude hexamethyldisilazane, and a metal complex with empirical formula $Mn(NR_2)(OPh)$ is obtained in dimeric form:

$$2Mn(NR_2)_2 + 2PhOH + 2THF \rightarrow 2HNR_2 + Mn_2(\mu\text{-}OPh)_2(NR_2)_2(THF)_2(\mathbf{1}) \quad (1)$$

The replacement of NR_2^- ligand represents a decrease in steric congestion around the metal center, and results in the formation of a dimeric, four-coordinate THF adduct. Crystalline material was not obtained in the absence of THF. We speculate that, in the absence of capping ligands, the coordinative unsaturation results in the formation of non-crystalline coordination polymers. Related dimeric manganese complexes with organic oxides have been reported.[30]

The addition of 1 equiv of the sterically encumbered 2,6-diphenylphenol ($Ph_2C_6H_3OH$) to $Mn(NR_2)_2$ also results in the isolation of a heteroleptic amido-phenolato dimer, but without terminal THF ligands:[31]

$$2Mn(NR_2)_2 + 2Ph_2C_6H_3OH \rightarrow 2HNR_2 + Mn_2(\mu\text{-}OC_6H_3Ph_2)_2(NR_2)_2(\mathbf{2}) \quad (2)$$

Isolation of the THF adduct of **2** has not been achieved. While the steric bulk of the large $Ph_2C_6H_3O^-$ ligand allows replacement of the NR_2^- ligand, it does not provide space enough for the coordination of a fourth THF ligand, as is observed in the formation of **1**. Isolation of the product in the presence of THF or Et_2O results in replacement of both amide ligands, and isolation of the monomeric $Mn(OC_6H_3Ph_2)_2(L)_2$ complex:

$$Mn(NR_2)_2 + 2Ph_2C_6H_3OH \rightarrow 2HNR_2 + Mn(OC_6H_3Ph_2)_2(L)_2(\mathbf{3}) \quad (L = THF, Et_2O) \quad (3)$$

The steric bulk of the $Ph_2C_6H_3O^-$ ligand most likely precludes the binding of THF, unless further steric strain is relieved by additional protolytic replacement of the remaining large NR_2^- ligands. Even under conditions stoichiometric for the formation of dimeric **2** (i.e., 1:1 Mn:Phenol), only monomeric **3** is isolated, suggesting that, in ligating ether solutions, **2** disproportionates to a significant degree into $Mn(NR_2)_2$ and **3** to relieve steric strain. Thus, the use of steric modifications to the bridging ligand controls coordination number (3 vs 4), and nuclearity (2 vs 1).

Given the drastic difference between the sterics of the phenyl and 2,6-diphenylbenzene groups, we explored the behavior of the sterically intermediate 2,4,6-trimethyl (mesityl) phenol (MesOH). To our surprise, the use of this phenol derivative resulted in the formation of the larger linear trinuclear cluster **4**:

$$3Mn(NR_2)_2 + 4PhOH + 2THF \rightarrow 4HNR_2 + Mn_3(\mu\text{-}OMes)_4(NR_2)_2(THF)_2(\mathbf{4}) \quad (4)$$

Though an increase in nuclearity from complex **1** to **4** resulting from enhanced steric bulk on the aryloxide ligands (Ph vs Mes) may seem surprising at first, careful consideration of the geometric features of the cluster explains the observation. In comparison to phenolate, the presence of methyl groups on the $MesO^-$ ligand increases the steric bulk sufficiently to preclude formation of the THF-bound dimer analogous to **1**, but not enough to stabilize the coordinatively unsaturated 3-coordinate dimer analogous to **2**. Indeed, we have not isolated either of these structure types with the mesityl group. Rather, the increased steric strain is relieved by the displacement of additional NR_2 ligands, which are larger than the $MesO^-$ ligands, resulting in formation of the trinuclear cluster. Thus, replacement of 4 of the 6 amide ligands on 3 equiv of $Mn(NR_2)_2$ results in a system wherein the central metal atom experiences the least steric strain due to the perpendicular stacking of the arene groups. A spacefilling model demonstrates the terminal THF/amide bound metals to possess the steric burden, in comparison to the central metal ligated by mesityloxide (Figure 2). Thus, in the intermediate sterics of complex **4**, the steric strain is relieved by the replacement of extra NR_2 ligands, which leaves sufficient room for aggregation to a trinuclear cluster, and binding of terminal THF ligands. A related 3-coordinate homoleptic trinuclear cluster using isopropoxide bridging and terminal ligands was reported by Power,[32a] and a siloxide-bridged trinuclear cluster with the same terminal NR_2 ligands was reported by Roesky et al.[32b]

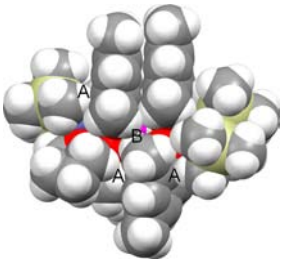

Figure 2. Spacefilling model of cluster **4** demonstrating steric relief by stacking of central aryloxides. Steric congestion between the arenes and the terminal ligands (THF, NR_2^-) (labeled "A") forces the arenes into an orientation in which they are approximately perpendicular to their respective Mn−O rhombs. This orientation results in a steric clash between the mesityl groups on neighboring rhombs. This interaction is labeled "B", and distorts the geometry about the central Mn atom toward the square planar geometry (τ_4 = 0.57).[33].

Reactivity with Water: Preparation of an Octanuclear Mn−O Cluster from Hydrolysis of Amide Ligands. In the interest of generating novel manganese−oxo clusters inspired by photosystem II, we have been exploring the use of H_2O as an acidic source for oxo ligands. Addition of excess liquid water to a colorless THF solution of **1** results in turbidity, and a slight

dx.doi.org/10.1021/ic202448c | Inorg. Chem. 2012, 51, 10095−10104

Table 1. Sample, Crystal, and Refinement Data for Reported Compounds

	1	2	3a	3b	4	5
chemical formula	$C_{32}H_{62}Mn_2N_2O_4Si_4$	$C_{49}H_{64}Cl_2Mn_2N_2O_2Si_4$	$C_{44}H_{43}MnO_4$	$C_{44}H_{48}MnO_4$	$C_{56}H_{106}Mn_3N_2O_6Si_4$	$C_{96}H_{108}Mn_8O_{20}$
fw	761.08	1006.16	690.72	695.76	1180.61	2021.34
T	293(2) K	173(2) K	100(2) K	173(2) K	173(2) K	173(2) K
wavelength	0.710 73 Å	0.710 73 Å	0.710 73 Å	0.710 73 Å	0.710 73 Å	0.710 73 Å
cryst size	0.080 × 0.210 × 0.320 mm^3	0.150 × 0.500 × 0.600 mm^3	0.100 × 0.200 × 0.300 mm^3	0.100 × 0.180 × 0.250 mm^3	0.050 × 0.150 × 0.200 mm^3	0.050 × 0.090 × 0.180 mm^3
cryst syst	triclinic	monoclinic	triclinic	triclinic	monoclinic	monoclinic
space group	$P\bar{1}$	$P2/n$	$P\bar{1}$	$P\bar{1}$	$C2/c$	Cc
unit cell dimensions	a = 8.8769(7) Å	a = 19.7255(14) Å	a = 9.419(4) Å	a = 10.8698(5) Å	a = 10.1362(17) Å	a = 26.479(3) Å
	b = 10.9042(8) Å	b = 12.6112(9) Å	b = 12.287(6) Å	b = 11.5942(6) Å	b = 32.734(6) Å	b = 45.599(6) Å
	c = 12.3175(9) Å	c = 20.9188(15) Å	c = 16.220(7) Å	c = 16.1014(8) Å	c = 19.570(3) Å	c = 20.072(3) Å
	α = 97.530(2)°	α = 90°	α = 97.956(8)°	α = 75.8960(10)°	α = 90°	α = 90°
	β = 106.0430(10)°	β = 92.6810(10)°	β = 91.959(9)°	β = 83.3060(10)°	β = 95.529(3)°	β = 129.425(2)°
	γ = 107.005(2)°	γ = 90°	γ = 111.792(9)°	γ = 70.1170(10)°	γ = 90°	γ = 90°
V	1066.23(14) $Å^3$	5198.1(6) $Å^3$	1718.7(13) $Å^3$	1849.46(16) $Å^3$	6463.1(19) $Å^3$	18721.(4) $Å^3$
Z	1	4	2	2	4	8
density (calcd)	1.185 Mg/cm^3	1.286 Mg/cm^3	1.335 Mg/cm^3	1.249 Mg/cm^3	1.213 Mg/cm^3	1.434 Mg/cm^3
abs coeff	0.737 mm^{-1}	0.719 mm^{-1}	0.429 mm^{-1}	0.399 mm^{-1}	0.696 mm^{-1}	1.110 mm^{-1}
data/restraints/params	5028/0/205	12 434/6/590	8060/0/443	14 067/0/446	7731/0/330	32 503/616/2348
GOF (S^a) on F^2	1.154	1.049	0.979	1.017	0.955	1.018
final R indices $I > 2\sigma(I)^b$	R1 = 0.0408, wR2 = 0.0958	R1 = 0.0294, wR2 = 0.0711	R1 = 0.0554, wR2 = 0.1266	R1 = 0.0482, wR2 = 0.1128	R1 = 0.0573, wR2 = 0.1166	R1 = 0.0529, wR2 = 0.1170
all data	R1 = 0.0548, wR2 = 0.1089	R1 = 0.0368, wR2 = 0.0767	R1 = 0.0946, wR2 = 0.1445	R1 = 0.0856, wR2 = 0.1294	R1 = 0.1397, wR2 = 0.1444	R1 = 0.0914, wR2 = 0.1373

$^a S = [\Sigma w(F_{obs}^2 - F_{calc}^2)^2/(m-n)]^{1/2}$. $^b R1 = (\Sigma||F_{obs}| - |F_{calc}||)/\Sigma|F_{obs}|$; $wR2 = [(\Sigma w(F_{obs}^2 - F_{calc}^2)^2)/\Sigma w F_{obs}^2]^{1/2}$ (across 2 columns).

darkening of solution upon heating. Crystallization from pentane diffusion results in clear, colorless crystals of a different morphology and unit cell than **1**. X-ray structure solution of this material identifies it as an octanuclear cluster, $Mn_8(\mu_5\text{-}O)_2(\mu\text{-}OPh)_{12}(THF)_6$ (**5**). The reaction presumably proceeds by protolytic replacement of NR_2^- ligands to give the Mn−O−OPh cluster and HNR_2, and rearrangement of the Mn-based fragments to give the octanuclear cluster:

$$6Mn_2(\mu\text{-}OPh)_2(NR_2)_2(THF)_2(\mathbf{1}) + 2H_2O \rightarrow Mn_8(\mu_5\text{-}O)_2(\mu\text{-}OPh)_{12}(THF)_6(\mathbf{5}) + 4HNR_2 + 4Mn(NR_2)_2 \quad (5)$$

The balanced chemical equation implies the regeneration of $Mn(NR_2)_2$ by mass balance, which is presumed to further hydrolyze with water to give $Mn(OH)_2$ and hexamethyldisilazane; The formation of $Mn(OH)_2$ is consistent with observed turbidity during reaction. This octanuclear cluster can also be formed directly from $Mn(NR_2)_2$, PhOH, and water without the need for isolation of precursor **1**. The stability of **5** in the presence of excess reactant water is encouraging, and illustrates the feasibility of preparation of unchelated manganese complexes with reduced coordination number, which are not protolytically destroyed in the presence of water.

X-ray Crystallography. Crystallographic data are given in Table 1, and selected metrics are described in Tables 2 and 3. Initial X-ray structure solutions of **1** gave large Fourier difference peaks attributed to stacking faults. These crystal flaws are a result of a low-temperature phase transition encountered upon cooling. Improved data sets for **1** were therefore obtained at room temperature. The structure of **1** indicates a single molecule per unit cell residing on a crystallographic center of inversion (Figure 3). The molecule can be described as a dimer of Mn atoms bridged by the oxygen atoms of the phenolate ligands. The manganese atoms are each terminally coordinated by a NR_2 and a THF ligand, with the entire cluster exhibiting a crystallographically imposed *trans* geometry, as the molecule is located on a crystallographic inversion center; it is likely that the *cis* geometry also exists in

Table 2. Selected Metrics[a] for $Mn_2(\mu\text{-}OPh)_2(NR_2)_2(THF)_2$ (1), $Mn_2(\mu\text{-}OC_6H_3Ph_2)_2(NR_2)_2$ (2), and $Mn_3(\mu\text{-}OC_6H_3Ph_2)_4(NR_2)_2(THF)_2$ (4)

	1[b]	2	4
Mn(1)−O(1/2)	2.0680(14)/2.0987(15)	2.0885(9)/2.0615(9)	2.084(2)/2.101(2)
Mn(2)−O(1/2)	2.0987(15)/2.0680(14)	2.0833(9)/2.0537(10)	2.060(2)/2.066(2)
Mn(1/2)−N(1/2)	2.0106(17)/2.0106(17)	1.9870(11)/1.9821(12)	2.015(3)/NA
Mn(1)−O(3)	2.1523(18)	NA	2.171(2)
O(1)−Mn(1/2)−O(2/2)	79.33(6)/79.33(6)	76.17(4)/76.45(4)	79.26(9)/80.62(8)/
N(1/2)−Mn(1/2)−O(1)	127.46(7)/137.17(7)	123.51(4)/128.09(4)	129.17(11)/NA
N(1/2)−Mn(1/2)−O(2)	137.17(7)/127.46(7)	139.67(4)/138.58(5)	132.21(10)/NA
O(1/2)−Mn(1)−O(3)	108.03(7)/91.62(7)	NA	103.92(9)/104.83(9)
N(1)−Mn(1)−O(3)	106.70(7)	NA	103.35(10)

[a]Divided entries refer to separate, related atoms and their associated metrics in the order given, e.g., O(1)−Mn(1/2)−O(2) denotes 3 angles, O(1)−Mn(1)−O(2) and O(1)−Mn(2)−O(2), and N(6)−Mn(1)−N(2). [b]Atoms numbered "1" and "2" are symmetry equivalents, are numbered such for consistency with the other structures, and are numbered differently in the Supporting Information.

dx.doi.org/10.1021/ic202448c | Inorg. Chem. 2012, 51, 10095−10104

Table 3. Selected Metrics[a] for Structure of $Mn_8(\mu_5\text{-}O)_2(\mu\text{-}OPh)_{12}(THF)_6$ (5)

	5
Mn(1/1/2/2)−O(1/2/1/2)	2.069(7)/2.279(7)/2.286(7)/2.079(7)
Mn(3/4/6/7)−O(1/1/2/2)	2.130(7)/2.123(8)/2.096(7)/2.151(8)
Mn(1/5/2/8)−O(13/13/23/23)	2.116(7)/2.054(7)/2.150(7)/2.010(7)
Mn(1/6/1/7)−O(11/11/12/12)	2.108(7)/2.065(8)/2.139(8)/2.067(8)
Mn(2/3/2/4)−O(21/21/22/22	2.099(7)/2.090(8)/2.104(8)/2.065(8)
Mn(3/5/4/5)−O(50/50/40/40)	2.096(7)/2.072(6)/2.087(8)/2.067(8)
Mn(6/8/7/8)−O(80/80/70/70)	2.136(7)/2.072(7)/2.088(7)/2.075(7)
Mn(3/4/5)−O(3/4/5)	2.178(7)/2.191(7)/2.224(6)
Mn(6/7/8)−O(6/7/8)	2.152(6)/2.230(7)/2.182(6)
Mn(1/1/2)···Mn(2/5/8)	2.9296(12)/3.080(2)/3.068(2)
Mn(1/1/8/8/)···Mn(6/7/6/7)	3.150(2)/3.154(2)/3.136(2)/3.151(2)
Mn(2/2/5/5/)···(Mn(3/4/3/4)	3.119(2)/3.168(3)/3.1470(19)/3.177(2)
O(1/1/2)···O(2/13/23)	3.231(6)/2.921(8)/2.927(8)
O(1)···O(21/22/40/50)	2.884(9)/2.814(9)/2.809(12)/2.876(10)
O(2)···O(11/12/70/80)	2.836(9)/2.866(10)/2.854(11)/2.875(10)
O(1/1/1/2)−Mn(1/1/2/2)−O(2/13/2/23)	95.9(2)/88.5(3)/95.4(2)/87.6(3)
O(1)−Mn(3)−O(21/30/50)	86.2(3)/86.2(3)/85.8(2)
O(1)−Mn(4)−O(22/30/40)	84.4(3)/85.9(3)/83.7(3)
O(2)−Mn(6)−O(11/60/80)	85.9(3)/86.6(3)/85.6(3)
O(2)−Mn(7)−O(12/60/70)	85.5(3)/84.2(3)/84.6(3)
O(1)−Mn(5)−O(13/40/50)	85.4(3)/81.1(3)/83.3(3)
O(2)−Mn(8)−O(23/70/80)	86.9(3)/82.8(3)/83.5(3)
Planarity[b]	
Mn(1/1/2), Mn(2/5/8), O(1/1/2), O(2/13/23)	0.0058/0.0062/0.0192
Mn(1), Mn(6/7), O(2), O(11/12)	0.1334/0.1699
Mn(2), Mn(3/4), O(1), O(21/22)	0.1676/0.1622
Mn(5), Mn(3/4), O(1), O(50/40)	0.0705/0.1055
Mn(8), Mn(6/7), O(2), O(70/80)	0.0974/0.1114
Mn(1), Mn(2), Mn(5), Mn(8), O(1), O(2), O(13), O(23)	0.0421

[a]Divided entries refer to separate, related atoms and their associated metrics in the order given, e.g., O(1)−Mn(3)−O(21/30) denotes 2 angles, and O(1)−Mn(3)−O(21) and O(1)−Mn(3)−O(30). [b]Calculated as rms deviation of atoms from their least-squares-fitted plane.

equilibrium in solution but is not obtained in crystalline form. A number of structurally related 4-coordinate manganese−organic-oxide dimers are known.[30a,b] The bridging phenolate oxygens are slightly pyramidal, lying 0.27 Å above the plane defined by the two manganese atoms and the *ipso* carbon of the phenol ring. Mn−O bond distances are ca. 2.07 and 2.10 Å for the two bridging contacts, with terminal ligand distances of 2.01 and 2.15 Å for the Mn−N and Mn−O bonds, respectively. The Mn_2O_2 rhomb is slightly distorted with compression of the O−Mn−O bond angle to ca. 79°, and expansion of the Mn−O−Mn bond angle to 101°. The geometry around the metal atoms is a severely distorted tetrahedron, perhaps better described as a pyramidalized trigonal manganese atom with THF coordinated axially. The Mn atom lies ca. 0.44 Å above the plane defined by the nitrogen, and the two bridging oxygen atoms.

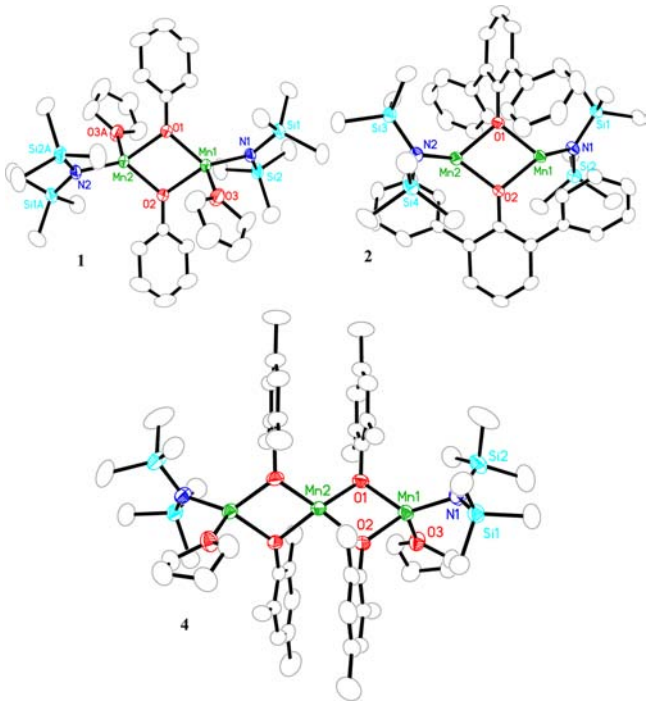

Figure 3. Structure of $Mn_2(\mu\text{-}OPh)_2(NR_2)_2(THF)_2$ (**1**) with ellipsoids at 30% probability, $Mn_2(\mu\text{-}OC_6H_3Ph_2)_2(NR_2)_2$ (**2**) with ellipsoids at 50% probability, and $Mn_3(\mu\text{-}OC_6H_3Ph_2)_4(NR_2)_2(THF)_2$ (**4**) with ellipsoids at 50% probability. Carbon atoms are shown as open ellipses. H-atoms omitted for clarity.

The structure of **2** (Figure 3) similarly exhibits a nearly planar Mn_2O_2 rhomb, with similar core bond distances of 2.06 and 2.08 Å, but with a greater bond angle distortion than that seen in the structure of **1**, with the O−Mn−O bond angles compressed to 76°, and the Mn−O−Mn bond angles widened to 104°. Unlike in the structure of **1**, the bridging oxygen atoms are nearly planar, deviating from the plane of the two manganese atoms and the aryl *ipso* carbon by only 0.06 Å. Unlike in the structure of **1**, the metal atoms are 3-coordinate, lacking the capping THF ligand. A related 3-coordinate manganese−organic-oxide dimer has been reported.[30c] The metal atom is pyramidalized, lying 0.48 Å above the plane defined by its ligand atoms. Each manganese comes in close proximity (2.65 Å) to a phenyl group, which may be responsible for the pyramidalization at Mn. The two diphenylphenol groups are oriented differently from one another, one being nearly perpendicular (82°) to the Mn_2O_2 rhomb, and the other forming a dihedral angle of 47° between the Mn_2O_2 rhomb and the central arene. This orientation allows interleaving of the pendant phenyl groups, and prevents a steric clash between phenyl groups on either side of the dimer core (Figure 4, left).

The structures of **3a** and **3b** (THF, and Et_2O complexes respectively) exhibit similar geometries about the metal centers. Mn−O bond lengths to the monoanionic diphenylphenol ligands are in the range 1.94−1.95 Å for both compounds, while the contacts to the neutral ether-based ligands are ca. 2.16 Å for **3a** and 2.18−2.19 Å for **3b**. Due to steric constraints the O−Mn−O bond angle between the diphenylphenol groups is expanded to 140° in the case of **3a** and 147° in the case of **3b**. The opposing bond angle between the ether ligands is compressed to 87° and 96° for **3a** and **3b**, respectively. The only major difference between the two structures is that the

dx.doi.org/10.1021/ic202448c | *Inorg. Chem.* 2012, 51, 10095−10104

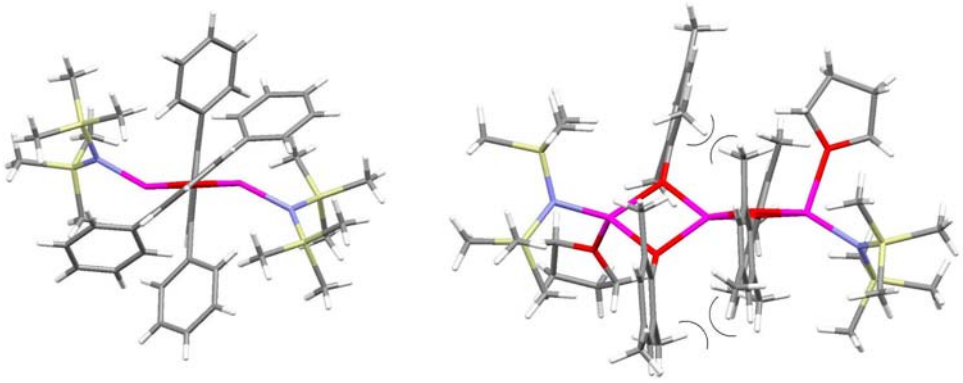

Figure 4. Top-down stick views of Mn−O rhombs. Rotational freedom of arenes in **2** permits interleaving (left). Hindered rotation of the arenes in **4** results in parallel stacked mestyl rings (right) and a steric clash (semicircles) between mesityl methyl groups, which distorts the central Mn geometry. (across 2 columns).

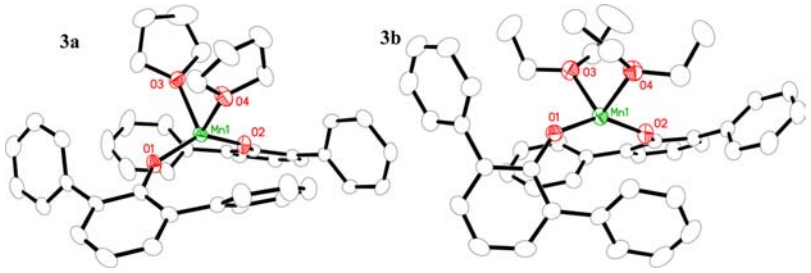

Figure 5. Structures of $Mn(OC_6H_3Ph_2)_2(THF)_2$ (**3a**) and $Mn(OC_6H_3Ph_2)_2(Et_2O)_2$ (**3b**) with ellipsoids at 50% probability. Carbon atoms are shown as open ellipses. H-atoms omitted for clarity.

$OC_6H_3Ph_2$ groups in **3b** have a "twist" which places the pendant phenyls of each ligand proximal to central arene of its neighbor, whereas the $OC_6H_3Ph_2$ groups of **3a** are of similar orientation and in direct opposition to one another (see Figure 5).

The core structure of **4** (Figure 3) is best described as two corner-fused Mn−O rhombs. The corner fusion at the central manganese resides on a crystallographic C_2 symmetry element. Related 3-coordinate homoleptic trinuclear clusters have been reported by the groups of Power and Roesky.[32] The rhombs exhibit similar angle distortion with the Mn−O−Mn angles compressed to ca. 80°, and the O−Mn−O angles widened to ca. 100°. Two of the bridging oxygens are pyramidalized, similar to that seen in **1** (0.35 Å above the plane defined by the *ipso* carbon and the two Mn atoms), while the other two are nearly planar, similar to that seen in **2** (0.03 Å above the analogous plane). The terminal manganese atoms exhibit 4-coordinate ligation, with the THF ligand occupying a fourth axial ligation site above the trigonal pyramid of the Mn atom. The increased steric congestion resulting from the methyl groups on the mesityl ring forces these arene groups to stack almost perfectly parallel to one another, and approximately perpendicular to their respective Mn_2O_2 rhombs (89° and 73°). As described in the previous section, this stacking results in the central Mn atom experiencing less steric congestion than the terminal Mn atoms, which are coordinated by THF and the bulky NR_2 ligands. However, this alignment of the arene rings restricts arene rotational freedom and precludes interleaving. This results in a steric clash between mesityl groups on the neighboring rhombs, as seen in the spacefilling model in Figure 2 (interaction B). The arene orientation in **4** is also illustrated in a top-down view of the Mn−O rhombs (Figure 4, right). The result of this strain is a 27° twist in the core structure such that the central Mn atom experiences a distortion away from the tetrahedral geometry toward the square planar geometry, a deviation from the expected 90° dihedral angle between the rhombs to ca. 63° (τ_4 value[33] = 0.57 compared with τ_4 = 0.68 for **1**).

The octanuclear cluster **5** crystallizes in the *Cc* space group, but possesses a noncrystallographic inversion center between the two molecules in the asymmetric unit. As a result, space group determination software (X-Prep) consistently and incorrectly selects *C*2/*c* as the most likely space group based upon intensity statistics. This noncrystallographic symmetry resulted in significant parameter correlation which was addressed using appropriate restraints. Complex **5** (Figure 6) exhibits a drastically different geometry than the low-coordinate Mn_8O_2 cluster reported by Wright,[27f] and represents a unique core in cluster chemistry. The central 4 Mn atoms are arranged in three edge-fused Mn−O rhombs with approximate trigonal bipyramidal geometry at the metal and oxygen atoms, and with the axial direction parallel to the long-axis of the molecule. The 4 central rhombs are nearly coplanar (rms deviation, 0.04 Å), and approximately square, with both the Mn and O bond angles in the range ca. 85−95°. The outermost Mn atoms are terminally ligated by one THF molecule each. The exterior oxygen atoms of these rhombs belong to PhO^- ligands, while the central two oxygen atoms are water-derived oxide. Each of these core oxides bridges to two more Mn atoms, which also have trigonal bipyramidal geometry, but with the primary axis oriented perpendicular to those in the central Mn and oxide atoms, and with the axial positions occupied by the core oxo and terminal THF ligands, and the equatorial positions occupied by bridging PhO^- ligands. The cluster possesses

dx.doi.org/10.1021/ic202448c | *Inorg. Chem.* 2012, 51, 10095−10104

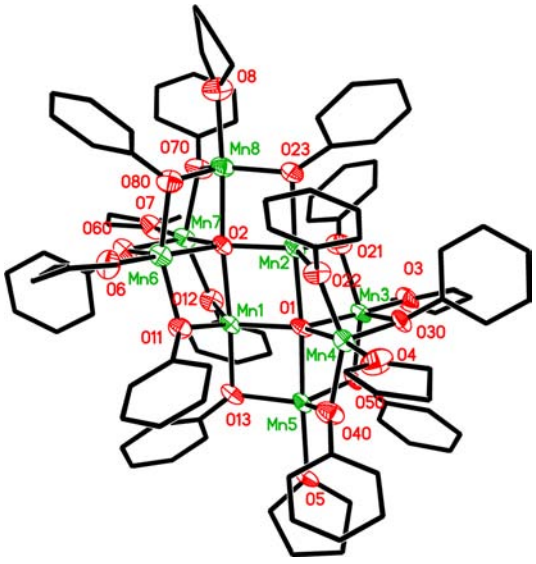

Figure 6. Structure of $Mn_8(\mu_5\text{-}O)_2(\mu\text{-}OPh)_{12}(THF)_6$ (**5**) with ellipsoids at 50% probability. Carbon atoms are shown in stick mode, and H-atoms are omitted for clarity.

approximate C_{2h} symmetry. To our knowledge, this cluster is the first example of an entirely unchelated all-Mn−O cluster core with coordination number exclusively less than 6.

Magnetic Measurements. The multinuclear clusters **4** and **5**, being composed of more than two manganese ions, were examined in more detail by magnetometry and EPR spectroscopy. Cluster **4** is a linear trinuclear cluster of high-spin manganese ions. Solid state magnetic data for crystalline **4** are presented in Figure 7. The slope of the Curie−Weiss plot in the region from 20 to 260 K gives a value of μ_{eff} of 9.98 Bohr magneton, consistent with three randomly oriented paramagnetic ions (theory = 10.25 Bohr magneton). The plot exhibits a Weiss constant of −16.3 K consistent with weak antiferromagnetic coupling of these ions, which couple below 10 K. Simulation of the magnetic data gives a coupling constant of $J = -1.2$ cm^{-1} (Figure 7, bottom).

Solid state magnetometry of compound **5** is presented in Figure 8. The Curie−Weiss plot exhibits two linear regions with a "kink" at approximately 85 K. The low temperature region fits well to a straight line whose slope corresponds to a μ_{eff} of 11.89 Bohr magneton, consistent with 4 randomly oriented (paramagnetic) $S = {}^5/_2$ ions (theory = 11.83 Bohr magneton). At temperatures above 90 K, complex **4** undergoes a phase transition to give a different Curie constant with μ_{eff} = 16.87, and a large negative Weiss constant of −99 K. This region of the plot is suggests 8 randomly oriented $S = {}^5/_2$ ions (theory =16.73 Bohr magneton) containing strong antiferromagnetic coupling. The two-phase magnetic behavior is consistent with the structure of cluster **5** which has two types of manganese ions: the four central rhomb ions, and the four peripheral ions (see Figure 6). At room temperature all 8 ions are randomly oriented. At low temperature, four of the manganese ions antiferromagnetically couple strongly, causing their spin contributions to cancel, leaving 4 randomly oriented $S = {}^5/_2$ ions.

EPR spectroscopy on crystalline octanuclear cluster **5** is consistent with the magnetic data. At low temperatures (3.6 K), the spectrum is an axial $S = {}^5/_2$ system with a zero-field splitting of ca. 500 G (Figure 9A, top). At elevated temperature, the

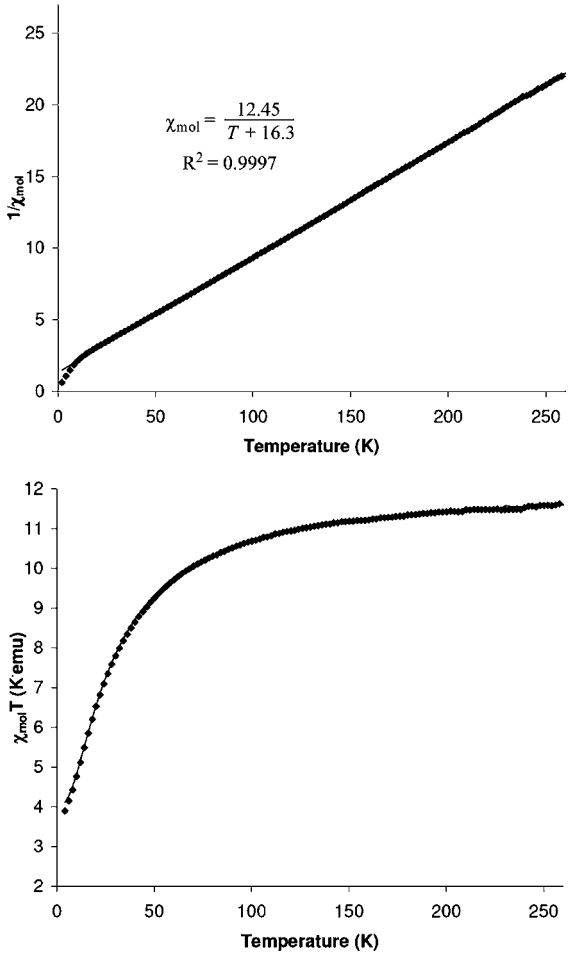

Figure 7. Magnetic data for crystalline **4**. Top: Curie−Weiss plot giving μ_{eff} = 9.98 μ_B, consistent with 3 paramagnetic $S = {}^5/_2$ ions (theory 10.24 μ_B) with a Weiss constant of −16.3 suggesting weak antiferromagnetic coupling. Bottom: Plot of χT vs T with simulation. g = 1.93, $J_{12} = J_{23} = -1.2$ cm^{-1}. The deviation of the magnetic data from the model at very low temperatures is due to the presence of a very small number of noninteracting impurity spins.

signal remains as an $S = {}^5/_2$ system, but with a change in signal geometry to that of an axially distorted isotropic $S = {}^5/_2$ signal centered around g = 2 (Figure 9A, bottom). At temperatures just above 4 K, the sharper axial signal initially broadens, and then becomes sharper as the temperature rises to 90 K. This temperature-dependent line shape of the EPR spectrum of **5** is illustrated in Figure 9B, and mirrors the magnetic data, which indicates a transition between two $S = {}^5/_2$ paramagnetic states. Very similar behavior is observed for **5** in solution, suggesting that the structure of **5** is retained when **5** is dissolved in toluene (see Supporting Information).

CONCLUDING REMARKS

Significant strides have been made in the exploration and structural characterization of manganese−oxo cluster chemistry in the past few decades. To enhance understanding of geometric rearrangement, and water binding and activation at such systems, manganese cluster systems with increased core lability and open coordination sites are needed. We have presented an Mn−O cluster with coordination number exclusively less than 6 and without chelation. These are attractive features for the design of systems which have both the

dx.doi.org/10.1021/ic202448c | Inorg. Chem. 2012, 51, 10095−10104

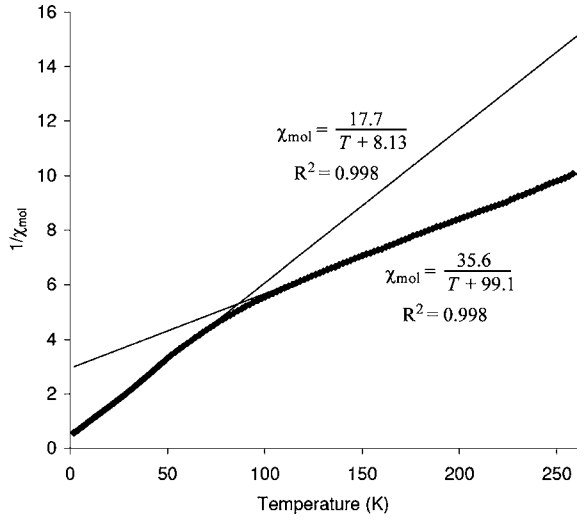

Figure 8. Magnetic data for crystalline **5**. Curie–Weiss plot giving μ_{eff} = 16.87 μ_B in the region 100–260 K, consistent with 8 paramagnetic $S = {}^5/_2$ ions (theory 16.73 μ_B) with a Weiss constant of −99.1 K suggesting strong antiferromagnetic coupling. In the region 2–70 K, the Curie–Weiss plot gives μ_{ff} = 11.89 μ_B consistent with 4 paramagnetic $S = {}^5/_2$ ions (theory 11.83 μ_B) with a Weiss constant of −8.13 K suggesting weak antiferromagnetic coupling.

ability to bind substrates to open coordination sites, and the lability to undergo facile chemical transformation. Despite the removal of stabilizing chelation and 6-coordination, the cluster is formed from (and stable to) dilute, solution-phase water. While the data do not directly support the presumed lability of the reported clusters, the lack of the entropic chelate effect is expected to labilize the reported systems, and favor reactive flexibility. Further studies exploring the reactivity of these systems, as well as the generation of new low-coordinate, unchelated systems with increased oxidation number, are planned in order to expand knowledge of this new class of cluster compounds.

EXPERIMENTAL SECTION

General Methods. All manipulations were performed under a dry, anaerobic N_2 atmosphere using Schlenk and glovebox techniques. Reagents and solvents were purchased from commercial vendors (Aldrich, Strem Chemicals), were of highest available purity, and were used without further purification unless otherwise noted. Anhydrous solvents such as pentane and dichloromethane (DCM) were purified using an Innovative Technology, Inc. Pure Solv system and stored in the glovebox over activated 4 Å molecular sieves for at least 24 h before use. Tetrahydrofuran (THF), ether (Et_2O), and hexamethyldisiloxane (HMDS) were distilled from sodium benzophenone ketyl under a nitrogen atmosphere and stored in the glovebox over 4-Å molecular sieves for 10 h. The synthesis of $Mn[N(SiMe_3)_2]_2$ was performed according to a published protocol.[29] ^{1}H NMR spectra were recorded on a Bruker Avance 400 MHz spectrometer with spectral width of 200 ppm. Values for chemical shifts (ppm) are referenced to the residual solvent proton resonances. Crystal diffraction data for all compounds were collected using a Bruker Kappa APEX II DUO diffractometer using Mo Kα radiation (λ = 0.710 73) from a fine-focused sealed tube. Data was collected at 100 K, 173 K, or room temperature, and structures were solved using direct methods. The X-ray data of compound **1** was collected at room temperature by coating crystal with epoxy. Further crystallographic information is available in the Supporting Information. Solid state magnetic measurements were carried out on a Quantum Design Model 6000 Physical Property Measurement System. Temperature was varied from 2 to 260 K at a constant field of 9998 Oe. The magnetic susceptibility was corrected

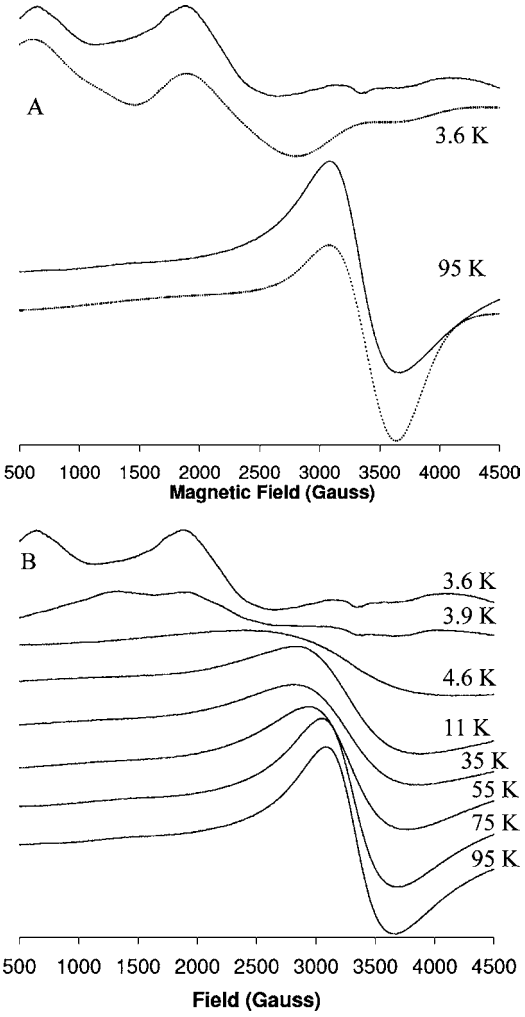

Figure 9. EPR spectra of crystalline **5**, MW freq 9.437, MW power = 2.012 mW, GHz, mod freq 100 kHz, mod amp 7 G: (A) spectral data (—) and simulation (---) of crystalline **5** at 3.6 K and 95 K; (B) temperature dependent EPR signals between 3.6 and 95 K.

for the diamagnetic contributions of the sample apparatus using experimentally determined temperature-independent diamagnetic susceptibility values, and for the diamagnetic ligands using Pascal's constants.[34] Magnetic data for compound **4** was simulated using JulX magnetic simulation software by E. Bill.[35] Elemental analyses were carried out under inert atmosphere by Midwest Microlab, LLC (Indianapolis, IN). EPR spectroscopy was performed using a Bruker EMX EPR spectrometer equipped with a liquid He cryostat. EPR data were simulated using the Bruker SimFonia software package.

Synthesis of $Mn_2(\mu\text{-}OPh)_2[N(SiMe_3)_2]_2(THF)_2$ (1). To a solution of $Mn[N(SiMe_3)_2]_2$ (188 mg, 0.502 mmol) in THF (5 mL) was added anhydrous phenol (47 mg, 0.50 mmol) in THF (5 mL). The resultant mixture is then transferred into a high-pressure flask, sealed under nitrogen atmosphere, and stirred at 70–75 °C. The solution turns from a white cloudy precipitate to black brown within the time course of 1–2 h. The reaction mixture is filtered, and filtrate is concentrated to ca. 3 mL under vacuum. Clear crystals were obtained at room temperature. The supernatant THF was decanted, and the crystals were rinsed with pentane and dried in vacuo. Yield: 0.083 g (44% based on Mn). Anal. Calcd for $C_{32}H_{62}Mn_2N_2O_4Si_4$: C, 50.50; H, 8.21; N, 3.68. Found: C, 49.99; H, 7.95; N, 3.69. ^{1}H NMR [ppm] (400 MHz, C_6D_6): δ −23 (v br), 9 (v br), 30 (v br), 33 (v br).

Synthesis of $[Mn_2(OC_6H_3Ph_2)_2[N(SiMe_3)_2]$ (2). A nonstoichiometric ratio of reactants was found to give the best purity in the synthesis of **2**.[31] $Mn[N(SiMe_3)_2]_2$ (0.20 g, 0.53 mmol) was dissolved in dichloromethane (5 mL) to which 2,6-diphenyl phenol (0.032 g, 0.13

dx.doi.org/10.1021/ic202448c | Inorg. Chem. 2012, 51, 10095–10104

mmol) is added. The resultant brown reaction mixture was stirred at room temperature for 1 h in nitrogen atmosphere. The solution is then filtered and concentrated to ca. 1 mL. The filtrate was crystallized at low temperature (−30 °C) by vapor diffusion method using hexamethyldisiloxane as vapor absorbent. The clear crystals were filtered after 2−3 days, washed with cold pentane, and dried in vacuo. Yield: 0.020 g, 33% based on Mn used). Anal. Calcd for $C_{48}H_{62}Mn_2N_2O_2Si_4$: C, 62.58; H, 6.78; N, 3.04. Found: C, 62.40; H, 6.45; N, 2.57.

Synthesis of $[Mn(OC_6H_3Ph_2)_2(THF)_2]$ (3a). The compound $Mn[N(SiMe_3)_2]_2$ (0.188 g, 0.50 mmol) was dissolved in 10 mL of dry tetrahydrofuran followed by addition of 2,6-diphenyl phenol (0.246 g, 1.00 mmol) stirred for 1 h. The resultant reaction mixture was filtered and concentrated to ca. 2 mL under vacuum and crystallized at low temperature (−30 °C) by using *n*-pentane (vapor diffusion technique). The clear crystals are filtered after 2−3 days and dried in vacuo for analyses. Yield: 0.185 g (53% based on Mn used). Anal. Calcd for $C_{44}H_{42}MnO_4$: C, 76.62; H, 6.14. Found: C, 76.18; H, 6.25. ^{1}H NMR [ppm] (400 MHz, C_6D_6): δ 4.5 (v br), 8 (v br), 33 (v br).

Synthesis of $[Mn(OC_6H_3Ph_2)_2(Et_2O)_2]$ (3b). The starting material $Mn[N(SiMe_3)_2]_2$ (0.187 g, 0.50 mmol) was dissolved in 10 mL of dry diethyl ether followed by addition of 2,6-diphenyl phenol (0.246 g, 1.00 mmol), stirred for 1 h. and filtered. The filtrate is kept at low temperature (−30 °C) from which white crystalline material appeared after two days. This was filtered and dried under vacuum for analysis. Yield: 0.22 g (64%). Anal. Calcd for $C_{44}H_{46}MnO_4$: C, 76.17; H, 6.68. Found: C, 76.20; H, 6.7.

Synthesis of $Mn_3[N(SiMe_3)_2]_2(OMes)_4(THF)_2$] (4). To a solution of $Mn[N(SiMe_3)_2]_2$ (188 mg, 0.502 mmol) in THF (5 mL) was added 2,4,6-trimethylphenol (68 mg, 0.50 mmol) in THF (5 mL). The resultant mixture is then transferred into a high-pressure vial, sealed under nitrogen atmosphere, and stirred at high temperature of 70−75 ° C. The solution turns from a cloudy precipitate to light brown within the time course of 1−2 h. Clear crystals were obtained after filtration and reduction of filtrate volume to ca. 1 mL. The crystals were collected by decanting, rinsing with pentane, and drying in vacuo. Yield: 0.095 g (49% based on Mn used). Anal. Calcd for $C_{56}H_{96}Mn_3N_2O_6Si_4$: C, 57.46; H, 8.27; N, 2.39. Found: C, 57.23; H, 7.97; N, 2.29. ^{1}H NMR [ppm] (400 MHz, C_6D_6): δ 12.2 (v br), 29 (v br), 33 (v br), 37.5 (v br).

Synthesis of $Mn_8(O)_2(OPh)_{12}(THF)_6$ (5). Method A: To a solution of $Mn[N(SiMe_3)_2]_2$ (188 mg, 0.502 mmol) in THF (5 mL) was added unpurified (wet) phenol (47 mg, 0.50 mmol) in THF (5 mL). The resultant mixture is then transferred into a high-pressure vial, sealed under nitrogen atmosphere, and stirred at high temperature of 90 °C. The solution turns first to cloudy white, and then to dark brown within the time course of 1−2 h. The reaction mixture is filtered, and filtrate is dried under vacuum. The dried residue is then redissolved in a small amount of THF. From this solution, clear crystalline material was obtained by vapor diffusion with pentane in 2−3 days. Yield: 0.028 g (22% based on Mn used). Anal. Calcd for $C_{88}H_{92}Mn_8O_{18}$: C, 56.31; H, 4.94. Found: C, 55.96; H, 5.20. ^{1}H NMR [ppm] (400 MHz, $CDCl_3$): δ 5.2 (v br), 30 (v br.), 36 (v br).

Method B: A (20 mg, 0.026 mmol) sample of **1** was dissolved in THF (15 mL) and to this mixture 5.0 μL of degassed DI water was added via syringe. The resultant mixture is then transferred into a high-pressure vial and sealed under nitrogen atmosphere and stirred at high temperature of 90 °C for two hours. The reaction mixture is filtered and filtrate is dried under vacuum. The dried residue is then redissolved in small amount of THF. From this solution, clear crystalline material was obtained by vapor diffusion with pentane in 2−3 days.

■ ASSOCIATED CONTENT

Supporting Information

Full crystallographic tables, crystallographic information files (CIF), NMR spectra, and EPR spectra of **5** in toluene. This material is available free of charge via the Internet at http://pubs.acs.org.

■ AUTHOR INFORMATION

Corresponding Author

*E-mail: mzdilla@temple.edu.

Notes

The authors declare no competing financial interest.

■ ACKNOWLEDGMENTS

We gratefully acknowledge Temple University for financial support of this work. Work at Princeton was supported by Grant DE-FG02-08ER45644. Dr. David Goldberg and Ms. Alison McQuilken are gratefully acknowledged for assistance with EPR measurements.

■ REFERENCES

(1) For some recent reviews, see: (a) McEvoy, J. P.; Brudvig, G. W. *Chem. Rev.* **2006**, *106*, 4455. (b) Renger, G.; Renger, T. *Photosynth. Res.* **2008**, *98*, 53. (c) Yano, J.; Yachandra, V. K. *Inorg. Chem.* **2008**, *47*, 1711.

(2) (a) Umena, Y; Kawakami, K.; Shen, J.-R.; Kamiya, N. *Nature* **2011**, *473*, 55. (b) Kawakami, K.; Umena, Y.; Kamiya, N.; Shen, J.-R. *Photochem. Photobiol.* **2011**, *104*, 9.

(3) For examples of XAS and EPR studies on the various S_n states of the OEC, see: (a) Roelofs, T. A.; Liang, W.; Latimer, M. J.; Cinco, R. M.; Rompel, A.; Andrews, J. C.; Sauer, K.; Yachandra, V. K.; Klein, M. *Proc. Natl. Acad. Sci. U.S.A.* **1996**, *93*, 3335. (b) Yachandra, V. K.; DeRose, V. J.; Latimer, M. J.; Mukerji, I.; Sauer, K.; Klein, M. P. *Science* **1993**, *260*, 675. (c) George, G. N.; Prince, R. C.; Cramer, S. P. *Science* **1989**, *243*, 789. (d) MacLachlan, D. J.; Hallahan, B. J.; Ruffle, S. V.; Nugent, J. H. A.; Evans, M. C. W.; Strange, R. W.; Hasnain, S. S. *Biochem. J.* **1992**, *285*, 569. (e) Guiles, R. D.; Zimmermann, J. L.; McDermott, A. E.; Yachandra, V. K.; Cole, J. L.; Dexheimer, S. L.; Britt, R. D.; Wieghardt, K.; Bossek, U. *Biochemistry* **1990**, *29*, 471. (f) Dismukes, G. C.; Siderer, Y. *Proc. Natl. Acad. Sci. U.S.A.* **1981**, *78*, 274. (g) Haddy, A.; Dunham, W. R.; Sands, R. H.; Aasa, R. *Biochim. Biophys. Acta* **1992**, *1099*, 25. (h) Lakshmi, K. V.; Eaton, S. S.; Eaton, G. R.; Frank, H. A.; Brudvig, G. W. *J. Phys. Chem. B* **1998**, *102*, 8327. (i) Messinger, J.; Robblee, J.; Yu, W. O.; Sauer, K.; Yachandra, V. K.; Klein, M. P. *J. Am. Chem. Soc.* **1997**, *119*, 11349. (j) Messinger, J.; Nugent, J. H. A.; Evans, M. C. W. *Biochemistry* **1997**, *36*, 11055.

(4) (a) Ferreira, K. N.; Iverson, T. M.; Maghlaoui, K.; Barber, J.; Iwatta, S. *Science* **2004**, *303*, 1831. (b) Zouni, A.; Witt, H. T.; Kern, J.; Fromme, P.; Krauss, N.; Saenger, W.; Orth, P. *Nature (London)* **2001**, *409*, 739. (c) Kamiya, N.; Shen, J. R. *Proc. Natl. Acad. Sci. U.S.A.* **2003**, *100*, 98. (d) Biesiadka, J.; Loll, B.; Kern, J.; Irrgang, K. D.; Zouni, A. *Phys. Chem. Chem. Phys.* **2004**, *6*, 4733. (e) Loll, B.; Kern, J.; Saegner, W.; Zouni, A.; Biesiadka, J. *Nature (London)* **2005**, *438*, 1040. (f) Guskov, A.; Kern, J.; Gabdulkhakov, A.; Broser, M.; Zouni, A.; Saenger, W. *Nat. Struct. Mol. Biol.* **2009**, *16*, 334.

(5) Mukhapadhyay, S.; Mandal, S. K.; Bhaduri, S.; Armstrong, W. H. *Chem. Rev.* **2004**, *104*, 3981.

(6) (a) Limburg, J.; Vrettos, J. S.; Liable-Sands, L. M.; Rheingold, A. L.; Crabtree, R. H.; Brudvig, G. W. *Science* **1999**, *283*, 1524. (b) Gao, Y.; Crabtree, R. H.; Brudvig, G. W. *Inorg. Chem.* **2012**, *51*, 4043.

(7) (a) Ruettinger, W. F.; Campana, C.; Dismukes, G. C. *J. Am. Chem. Soc.* **1997**, *119*, 6670. (b) Ruettinger, W. F.; Ho, D. M.; Dismukes, G. C. *Inorg. Chem.* **1999**, *38*, 1036. (c) Wu, J.-Z.; Sellitto, E.; Yap, G. P. A.; Sheats, J.; Dismukes, G. C. *Inorg. Chem.* **2004**, *43*, 5795. (d) Ruettinger, W.; Yagi, M.; Wolf, K.; Bernasek, S.; Dismukes, G. C. *J. Am. Chem. Soc.* **2000**, *122*, 10353. (e) Brimblecombe, R.; Swiegers, G. F.; Dismukes, G. C.; Spiccia, L. *Angew. Chem., Int. Ed.* **2008**, *47*, 7335. (f) Brimblecombe, R; Koo, A.; Dismukes, G. C.; Swiegers, G. F.; Spiccia, L. *J. Am. Chem. Soc.* **2010**, *132*, 2892.

(8) (a) Mishra, A.; Wernsdorfer, W.; Abboud, K. A.; Christou, G. *Chem. Commun.* **2005**, 54. (b) Mishra, A; Yano, J.; Pushkar, Y.; Yachandra, V. K.; Abboud, K. A.; Christou, G. *Chem. Commun.* **2007**, 1538. (c) Mukherjee, S.; Stull, J. A.; Yano, J.; Stamatatos, T. C.;

Pringouri, K.; Stich, T. A.; Abboud, K. A.; Britt, R. D.; Yachandra, V. K.; Christou, G. *Proc. Natl. Acad. Sci. U.S.A.* **2012**, *109*, 2257.
(9) Yang, P.-P.; Li, L.-C. *Inorg. Chim. Acta* **2011**, *371*, 95.
(10) Kanady, J. S.; Tsui, E. Y.; Day, M. W.; Agapie, T. *Science* **2011**, *333*, 733.
(11) Park, Y. J.; Ziller, J. W.; Borovik, A. S. *J. Am. Chem. Soc.* **2011**, *133*, 9258.
(12) (a) Kanan, M. W.; Nocera, D. G. *Science* **2008**, *321*, 1072. (b) Lutterman, D. A.; Surendranath, Y.; Nocera, D. G. *J. Am. Chem. Soc.* **2009**, *131*, 3838. (c) Surendranath, Y.; Dincă, M.; Nocera, D. G. *J. Am. Chem. Soc.* **2009**, *131*, 2615. (d) Dincă, M.; Surendranath, Y.; Nocera, D. G. *Proc. Natl. Acad. Sci. U. S. A.* **2010**, *107*, 10337.
(13) Kanan, M. W.; Yano, J.; Surendranath, Y.; Dinca, M.; Yachandra, V. K.; Nocera, D. G. *J. Am. Chem. Soc.* **2010**, *132*, 13692.
(14) Mukhopadhyay, S.; Mok, H. J.; Staples, R. J.; Armstrong, W. H. *J. Am. Chem. Soc.* **2004**, *126*, 9202.
(15) (a) Chen, H.; Faller, J. W.; Crabtree, R. H.; Brudvig, G. W. *J. Am. Chem. Soc.* **2004**, *126*, 7345. (b) Sarneski, J. E.; Thorp, H. H.; Brudvig, G. W.; Crabtree, R. H.; Schulte, G. K. *J. Am. Chem. Soc.* **1990**, *112*, 7255. (c) Chen, H.; Collomb, M.-N.; Duboc, C.; Blondin, G.; Riviere, E.; Faller, J. W.; Crabtree, R. H.; Brudvig, G. W. *Inorg. Chem.* **2005**, *44*, 9567. (d) Baffert, C.; Orio, M.; Pantazis, D. A.; Duboc, C.; Blackman, A. G.; Blondin, G.; Neese, F.; Deronzier, A.; Collomb, M.-N. *Inorg. Chem.* **2009**, *48*, 10281.
(16) Cox, N.; Rapatskiy, L.; Su, J.-H.; Pantazis, D. A.; Sugiura, M.; Kulik, L.; Dorlet, P.; Rutherford, A. W.; Neese, F.; Boussac, A.; Lubitz, W.; Messinger, J. *J. Am. Chem. Soc.* **2011**, *133*, 3635.
(17) Power, P. P. *J. Organomet. Chem.* **2004**, *689*, 3904.
(18) Holland, P. L. *Acc. Chem. Res.* **2008**, *41*, 905.
(19) Mindiola, D. J. *Angew. Chem., Int. Ed.* **2006**, *45*, 862.
(20) Iluc, V. M.; Miller, A. J. M.; Anderson, J. S.; Monreal, M. J.; Mehn, M. P.; Hillhouse, G. L. *J. Am. Chem. Soc.* **2011**, *133*, 13055.
(21) Cummins, C. C. *Angew. Chem., Int. Ed.* **2006**, *45*, 862.
(22) (a) Cantalupo, S. A.; Ferreira, H. E.; Bataineh, E.; King, A. J.; Petersen, M. V.; Wojtasiewicz, T.; DiPasquale, A. G.; Rheingold, A. L.; Doerrer, L. H. *Inorg. Chem.* **2011**, *50*, 6584. (b) Buzzeo, M. C.; Iqbal, A. H.; Long, C. M.; Millar, D.; Patel, S.; Pellow, M. A.; Saddoughi, S. A.; Smenton, A. L.; Turner, J. F. C.; Wadhawan, J. D.; Compton, R. G.; Golen, J. A.; Rheingold, A. L.; Doerrer, L. H. *Inorg. Chem.* **2004**, *24*, 7709. (c) Simpson, R. D.; Bergman, R. G. *Organometallics* **1993**, *12*, 781. (d) Snelgrove, J. L.; Conrad, J. C.; Eelman, M. D.; Moriarty, M. M.; Yap, G. P. A.; Fogg, D. E. *Organometallics* **2005**, *24*, 103. (e) Lionetti, D.; Medvecz, A. J.; Ugrinova, V.; Quiroz-Guzman, M.; Noll, B. C.; Brown, S. N. *Inorg. Chem.* **2010**, *49*, 4687. (f) Kriley, C. E.; Kerschne, J. L.; Fanwick, P. E.; Rothwell, I. P. *Organometallics* **1993**, *12*, 2051.
(23) As standard convention dictates, a "cluster" is defined as a multinuclear complex of metal nuclearity greater than 2.
(24) (a) Blake, A. J.; Harris, N. A.; Kays, D. L.; Lewis, W.; Moxey, G. J. *Acta Crystallogr., Sect. C* **2010**, *66*, m204. (b) Raptopoulou, C. P.; Boudalis, A. K.; Lazarou, K. N.; Psycharis, V.; Panopoulos, N.; Fardis, M.; Diamantopoulos, G.; Tuchagues, J. P.; Mari, A.; Papavassiliou, G. *Polyhedron* **2008**, *27*, 3575. (c) Kennedy, A. R.; Klett, J.; Mulvey, R. E.; Newton, S.; Wright, D. S. *Chem. Commun.* **2008**, 308. (d) Liu, Y.; Dou, J.; Niu, M.; Zhang, X. *Acta Crystallogr., Sect. E* **2007**, *63*, m2771. (e) Kitajima, N.; Osawa, M.; Tanaka, M.; Moro-oka, Y. *J. Am. Chem. Soc.* **1991**, *113*, 8952. (f) Al-Juaid, S. S.; Eaborn, C.; El-Hamruni, S. M.; Hitchcock, P. B.; Smith, J. D.; Can, S. E. S. *J. Organomet. Chem.* **2002**, *649*, 121. (g) Celenligil-Cetin, R.; Paraskevopoulou, P.; Lalioti, N.; Sanakis, Y.; Staples, R. J.; Rath, N. P.; Stavropoulos, P. *Inorg. Chem.* **2008**, *47*, 10998. (h) Mikata, Y.; So, H.; Yamashita, A.; Kawamura, A.; Mikuriya, M.; Fukui, K.; Ichimura, A.; Yano, S. *J. Chem. Soc., Dalton Trans.* **2007**, 3330. (i) Chai, J.; Zhu, H.; Stuckl, A. C.; Roesky, H. W.; Magull, J.; Bencini, A.; Caneschi, A.; Gatteschi, D. *J. Am. Chem. Soc.* **2005**, *127*, 9201. (j) Neuba, A.; Seewald, O.; Florke, U.; Henkel, G. *Acta Crystallogr., Sect. E* **2007**, *63*, m2099. (k) Mulvey, R. E.; Blair, V. L.; Clegg, W.; Kennedy, A. R.; Klett, J.; Russo, L. *Nat. Chem.* **2010**, *2*, 588.
(25) (a) Kasani, A.; Babu, R. P. K.; Feghali, K.; Gambarotta, S.; Yap, G. P. A.; Thompson, L. K.; Herbst-Irmer, R. *Chem.—Eur. J.* **1999**, *5*, 577. (b) Yang, C.-I.; Wernsdorfer, W.; Cheng, K.-H.; Nakano, M.; Lee, G.-H.; Tsai, H. L. *Inorg. Chem.* **2008**, *47*, 10184. (c) Viciano-Chumillas, M.; Tanase, S.; Mutikainen, I.; Turpeinen, U.; de Jongh, L. J.; Reedijk, J. *J. Chem. Soc., Dalton Trans.* **2009**, 7445.
(26) There are hundreds of examples; a few are: (a) Tasiopoulos, A. J.; Vinslava, A.; Wernsdorfer, W.; Abboud, K. A.; Christou, G. *Angew. Chem., Int. Ed.* **2004**, *43*, 2117. (b) Liu, C.-M.; Zhang, D.-Q.; Zhu, D.-B. *Chem. Commun.* **2008**, 368. (c) Stamatatos, T.; Foguet-Albiol, D.; Wernsdorfer, W.; Abboud, K. A.; Christou, G. *Chem. Commun.* **2011**, *47*, 274.
(27) (a) Baskar, V.; Shanmugam, M.; Sanudo, E. C.; Shanmugam, M.; Collison, D.; McInnes, E. J. L.; Wei, Q.; Winpenny, R. E. P. *Chem. Commun.* **2007**, 37. (b) Cotton, F. A.; Daniels, L. M.; Falvello, L. R.; Matonic, J. H.; Murillo, C. A.; Wang, X.; Zhou, H. *Inorg. Chim. Acta* **1997**, *266*, 91. (c) Gallo, E.; Solari, E.; De Angelis, S.; Floriani, C.; Re, N.; Chiesi-Villa, A.; Rizzoli, C. *J. Am. Chem. Soc.* **1993**, *115*, 9850. (d) Beagley, B.; McAuliffe, C. A.; MacRory, P. P.; Ndifon, P. T.; Pritchard, R. G. *Chem. Commun.* **1990**, 309. (e) Campora, J.; Palma, P.; Perez, C. M.; Rodriguez-Delgado, A.; Alvarez, E.; Gutierrez-Puebla, E. *Organometallics* **2010**, *29*, 2960. (f) Alvarez, C. S.; Bond, A. D.; Cave, D.; Mosquera, M. E. G.; Harron, E. A.; Layfield, R. A.; McPartlin, M.; Rawson, J. M.; Wood, P. T.; Wright, D. S. *Chem. Commun.* **2002**, 2980.
(28) (a) Rao, P. V.; Holm, R. H. *Chem. Rev.* **2004**, *104*, 527. (b) Link, H; Fenke, D. *Z. Anorg. Allg. Chem.* **1999**, *625*, 1878. (c) Verma, A. K.; Nazif, T. N.; Achim, C.; Lee, S. C. *J. Am. Chem. Soc.* **1999**, *122*, 11013.
(29) Anderson, R. A.; Faegri, K.; Green, J. C.; Haaland, A.; Lappert, M. F.; Leung, W.-P.; Rypdal., K. *Inorg. Chem.* **1988**, *27*, 1782.
(30) (a) Coucouvanis, D.; Greiwe, K.; Salifoglou, A.; Challen, P.; Simopoulos, A.; Kostikas, A. *Inorg. Chem.* **1988**, *27*, 593. (b) Bartlett, R. A.; Ellison, J. J.; Power, P. P.; Shoner, S. C. *Inorg. Chem.* **1991**, *30*, 2888. (c) Jones, R. A.; Koschmieder, S. U.; Nunn, C. M. *Inorg. Chem.* **1988**, *27*, 4524. (d) Bunge, S. D.; Bertke, J. A.; Cleland, T. L. *Inorg. Chem.* **2009**, *48*, 8037.
(31) While eq 2 suggests a 1:1 stoichiometry for the formation of **2**, we have found that use of excess $Mn(NR_2)_2$ results in isolated material of higher purity. We speculate that, in the presence of significant concentrations of Ph_2PhOH, additional amide protolysis results in a mixture of **2** along with homoleptic dimers or coordination polymers of $[Mn(OPh_2Ph)_2]$.
(32) (a) Murray, B. D.; Hope, H.; Power, P. P. *J. Am. Chem. Soc.* **1985**, *107*, 169. (b) Gosink, H.-J.; Roesky, H. W.; Schmidt, H.-G.; Noltemeyer, N.; Irmer, E.; Herbst-Irmer, R. *Organometallics* **1994**, *13*, 3420.
(33) Yang, L.; Powell, D. R.; Houser, R. P. *Dalton Trans.* **2007**, 955.
(34) Bain, G. A.; Berry, J. F. *J. Chem. Educ.* **2008**, *85*, 532.
(35) Bill, E. *JulX Magnetic Simulator*; http://www.mpibac.mpg.de/bac/logins/bill/julX_en.php (accessed July 18, 2012).